Dielectric and plasmonic vivaldi antennas for on-chip wireless communication

Published Version:
Calò G., Alam B., Bellanca G., Fuschini F., Barbiroli M., Tralli V., et al. (2019). Dielectric and plasmonic vivaldi antennas for on-chip wireless communication. IEEE [10.1109/ICTON.2019.8840426].

Availability:
This version is available at: https://hdl.handle.net/11585/728939 since: 2020-04-10

Published:

DOI: http://doi.org/10.1109/ICTON.2019.8840426

Dielectric and Plasmonic Vivaldi Antennas for On-chip Wireless Communication

Giovanna Calò, Badrul Alam, Gaetano Bellanca, Franco Fuschini*, Marina Barbiroli*, Velio Tralli**, Paolo Bassi*, Tiziana Stomeo***, Michele Bozzetti, Ali Emre Kaplan**, Jinous Shafiei Dehkordi**, Marco Zoli*, Jacopo Nanni*, and Vincenzo Petruzzelli**

Department of Electrical and Information Engineering, Polytechnic of Bari, Via E. Orabona, 4, 70125 Bari, Italy

**Dept. of Electrical, Electronic and Information Eng. "G. Marconi", University of Bologna, Viale Risorgimento, 2, 40136 Bologna, Italy*

***Dept. of Engineering, University of Ferrara, Via Saragat, 1, 44124 Ferrara, Italy*

**** Istituto Italiano di Tecnologia, Center for Biomolecular Nanotechnologies,, Via Barsanti, 73010 Arnesano (LE), Italy*

Tel: (+39) 0805963525, Fax: (+39) 0805963410, e-mail: vincenzo.petruzzelli@poliba.it

ABSTRACT
In this paper, different technologies enabling wireless on-chip communication are investigated. In particular, plasmonic Vivaldi antennas coupled to silicon waveguides and all-dielectric Vivaldi antennas are proposed. The design criteria and the performances of the two antenna configurations are also discussed.
Keywords: Plasmonic Vivaldi antenna, Dielectric antenna, Optical Wireless Network on Chip, silicon photonics, integrated optics.

1. INTRODUCTION

The development of chip multiprocessors (CMP) systems, for which hundreds or thousands of chips are integrated together, can lead to unprecedented computational resources. However, in such complex systems the data communication is a major challenge that finds limits (e.g. bandwidth, delay, power consumption) in the use of the classical electrical wires. One of the most promising solutions to overcome of the inter- and intra-chip communication bottleneck is the on-chip integration of photonic components [1]. A large number of integrated photonic and plasmonic devices have been proposed as building blocks for routing the signal in complex photonic networks [1-4].

Another alternative technology for on-chip communication is the Wireless Network on Chip (WiNoC), which addresses the scalability limitations of electrical and optical multi-hop networks on chip (NoC) [5, 6]. The advantages of on-chip wireless communication, demonstrated in the millimeter-wave range, can be conjugated with the performances of the optical communication through the wireless transmission of optical signals. Optical WiNoCs (OWiNoCs) can allow to achieve integrability and compatibility with already present optical networks, as well as signal transparency. The recent development of optical and plasmonic antennas, integrated with standard silicon waveguides and having high gain in the longitudinal directions, is paving the way for the on-chip wireless communication [7- 9].

In this paper, we propose two different configurations of integrated antennas based on silicon waveguides and compatible with standard CMOS technology. The first structure is a plasmonic Vivaldi antenna coupled to a silicon waveguide, whereas the second one is an all-dielectric Vivaldi antenna. The design criteria and the performances of the two antennas are described in the following.

2. PLASMONIC AND DIELECTRIC VIVALDI ANTENNAS

The two antenna configurations proposed in this paper are shown in Fig. 1. In particular, Fig. 1 (a) schematizes the plasmonic Vivaldi antenna coupled to a silicon waveguide. The optical signal, launched in input to the Si waveguide, is vertically coupled to the plasmonic slot waveguide through a hybrid (Si-Au) coupling section. After the coupling section, the plasmonic slot waveguide opens according to a Vivaldi profile and radiate the signal in the surrounding medium (considered as homogeneous) with refractive index n_{SiO2}=1.445. The relevant geometrical parameters are highlighted in Fig. 1 (a). In particular, the height of the Si waveguide was fixed to the standard value h=220 nm, whereas the value of the gap between the silicon and the plasmonic waveguide is equal to g=80 nm and the slot gap is equal to s=60 nm. The other geometrical parameters were chosen according to the design procedure that will be described in the following. The configuration shown in Fig. 1 (a) is similar to the one proposed in [8] by the authors, but here gold is used for the plasmonic slot waveguide owing to its higher chemical stability with respect to silver. Moreover, less strict fabrication constraints are imposed by the slot gap value s=60 nm.

The second Vivaldi antenna configuration, shown in Fig. 1 (b), is all-dielectric and it is made of a tapered silicon waveguide with directors shaped according to a Vivaldi profile. Also in this case, the structure is embedded in a homogeneous medium with refractive index n_{SiO2}=1.445. Moreover, the standard values for the height h=220 nm and for the width w_D=450 nm of the Si waveguide were fixed, and the taper length L_T=10 μm was chosen as in [7]. The other geometrical parameters were designed according to the procedure described in the following.

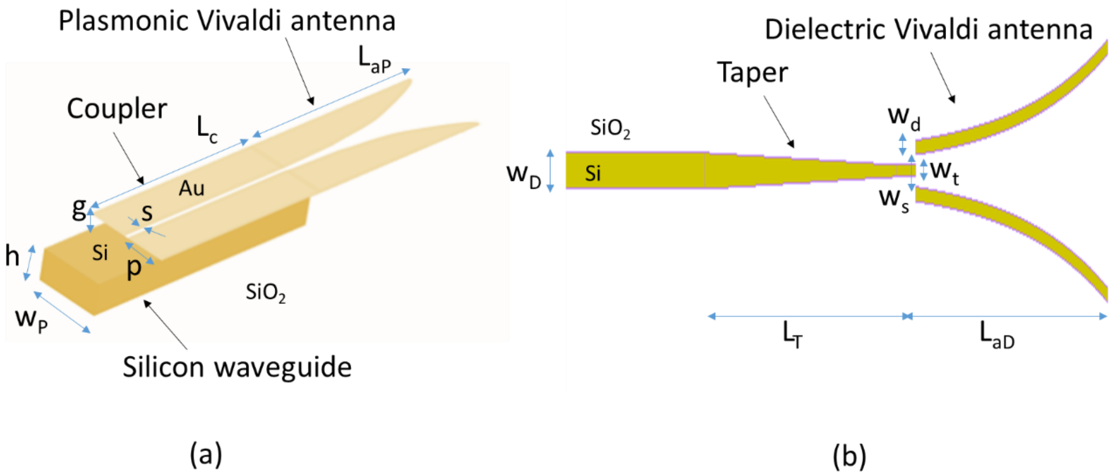

Figure 1. Schemes of (a) the plasmonic Vivaldi antenna coupled to a silicon waveguide through a hybrid Si-Au directional coupler, and (b) the all-dielectric Vivaldi antenna made of a tapered silicon waveguide with Vivaldi-shaped directors.

2.1 Design of the plasmonic Vivaldi antenna

The design of the plasmonic Vivaldi antenna coupled to the Si waveguide was obtained according to the procedure described in [8, 9]. For the sake of self-consistency, we summarize here the main steps of the design methodology. The hybrid Si-Au coupler feeding the plasmonic Vivaldi antenna was designed according to the coupled mode theory (CMT) and the normal mode analysis [3], and the results were validated with the full-wave Finite Difference Time Domain (FDTD) simulations [10]. According to the CMT, the synchronism condition (i.e. equal effective refractive indices) between the modes of the Si and the Au slot waveguides, considered as isolated, must be achieved to guarantee the total transfer of power. For this purpose, we have chosen to variate the widths of the two waveguides, i.e. the w_P and p parameters in Fig. 1 (a).

Fig. 2 (a) shows the width p of the plasmonic waveguide, which guarantees the synchronism condition, as a function on the corresponding Si waveguide width w_P. The gap of the slotted plasmonic waveguide is s = 60 nm and the gold layer thickness is t= 30 nm. Each point (p, w_P) of this design curve corresponds to possible couples of values of waveguide widths that guarantee the total power transfer between the dielectric and the plasmonic waveguides. In this paper, we have chosen p=228 nm and w_P=320 nm corresponding to the red dot in Fig. 2 (a). The corresponding value of the coupling length L_c=1670 nm was calculated according to the CMT from the equation $L_c=\lambda/(n_{c1}-n_{c2})$, where n_{c1} and n_{c2} are the effective refractive indices of the first two normal modes of the overall hybrid coupler.

The plasmonic antenna width value, which is equal to p=228 nm, is constrained by the design of the coupler. Therefore, the antenna radiation characteristics were optimized considering only the variation of the antenna length L_{aP}. Fig. 2 (b) shows the antenna maximum directivity D (red curve) and gain G (blue curve) as a function of the antenna length L_{aP}. Standard near-to-far field projections of the fields recorded on a closed box, surrounding the antenna and the coupled waveguide, were calculated after the Fourier transformation of the time-domain electromagnetic field. It is worth highlighting that the gain accounts for the radiation efficiency and, therefore, it includes the coupler efficiency and the material losses (either dielectric or conduction losses). Conversely, the directivity gives information on the radiation characteristics of the antenna itself, regardless of the coupler and of the radiation efficiency. As we can see from Fig. 2(b), the antenna maximum gain is lower than the corresponding directivity especially owing to the metal losses. From Fig. 2 (b) we have chosen the optimal value of the antenna length L_{aP}=2 μm which maximizes the gain.

2.2 Design of the dielectric Vivaldi antenna

The dielectric Vivaldi antenna was designed through parametric analysis. A number of FDTD simulations were performed to choose the optimal values of the director width w_d=180 nm and of the taper tip width w_t=150 nm, which guarantee higher directivity D and gain G values. It is worth pointing out that, in the case of the all-dielectric antenna, the directivity and the gain are almost equal since the Si losses are negligible.

Fig. 3 (a) shows the maximum gain G for the all-dielectric antenna as a function of the director distance w_s for the all-dielectric antenna with antenna length L_{aD}=15 µm. From Fig. 3 (a) we have chosen the value w_s=400 nm, since a further increase of the director distance does not correspond to a significant increase of the maximum gain. Fig. 3 (b) shows the maximum gain G as a function of the antenna length L_{aP} for the all-dielectric antenna with director distance w_s= 400 nm. From Fig. 3 (b) we can infer that, given all the other geometrical parameters, the optimal length of the antenna is L_{aD}=15 µm.

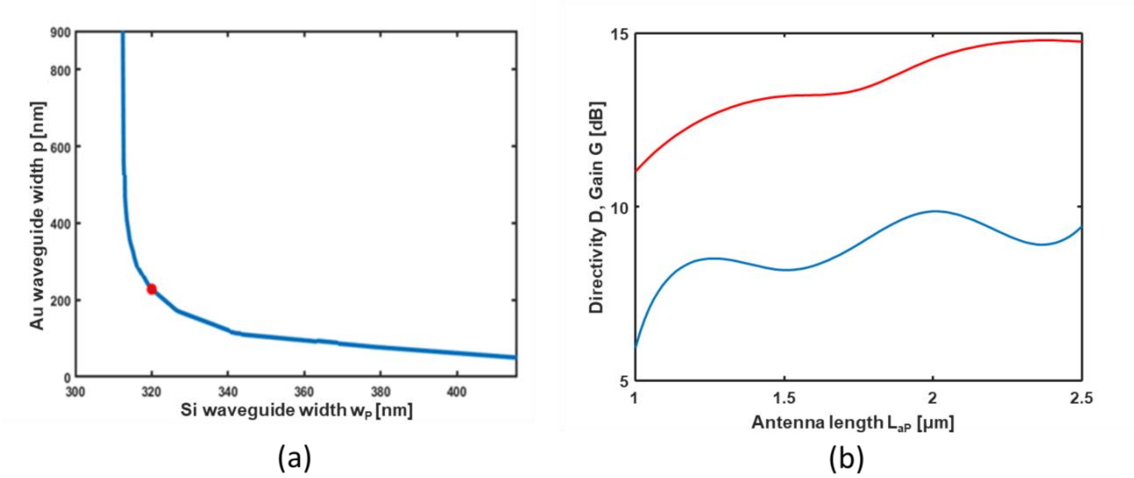

Figure 2. (a) Width p of the plasmonic waveguide, which guarantees the synchronism condition, as a function of the corresponding Si waveguide width w_P. The curve was calculated according to the CMT. The red dot denotes the values, w_P=320 nm and p=228 nm, chosen for the antenna design. (b) Directivity D (red curve) and gain G (blue curve) of the plasmonic Vivaldi antenna coupled to the Si waveguide as a function of the antenna length L_{aP}. The curves were calculated by the FDTD simulations.

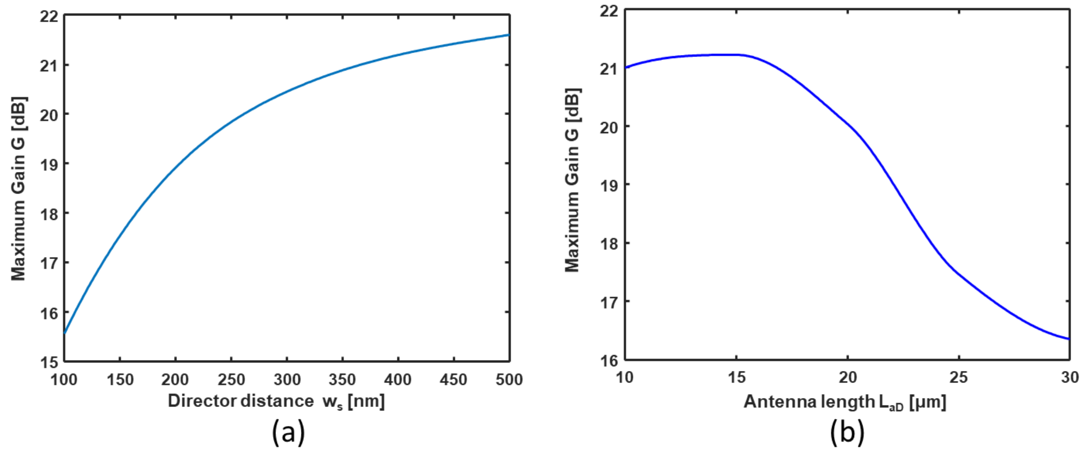

Figure 3. (a) Maximum gain G as a function of the director distance w_s for the all-dielectric antenna with antenna length L_{aD}=15 µm. (b) Maximum gain G as a function of the antenna length L_{aD} for the all-dielectric antenna with director distance w_s= 400 nm. The other geometrical parameters are taper tip width w_t=150 nm, taper length L_T=10 µm, director width w_d=180 nm. The two curves were calculated by the FDTD simulations.

2.3 Radiation diagrams

Figs. 4 (a) and (b) show the gain G as a function of the angles φ with fixed value of θ=90° (Fig. 4 a) and of θ by fixing φ=0° (Fig. 4 b) for the plasmonic Vivaldi antenna (black curves) and the all-dielectric Vivaldi antenna (blue curves).

The curves in Fig. 4 were obtained by the FDTD simulations and by near-to-far field projections of the fields recorded on a closed box, surrounding the antenna. The calculated half-power beam-widths are $\Delta\theta_{3dB}$=35° and $\Delta\varphi_{3dB}$=32° for the plasmonic antenna and $\Delta\theta_{3dB}$=13° and $\Delta\varphi_{3dB}$=12° for the all-dielectric one.

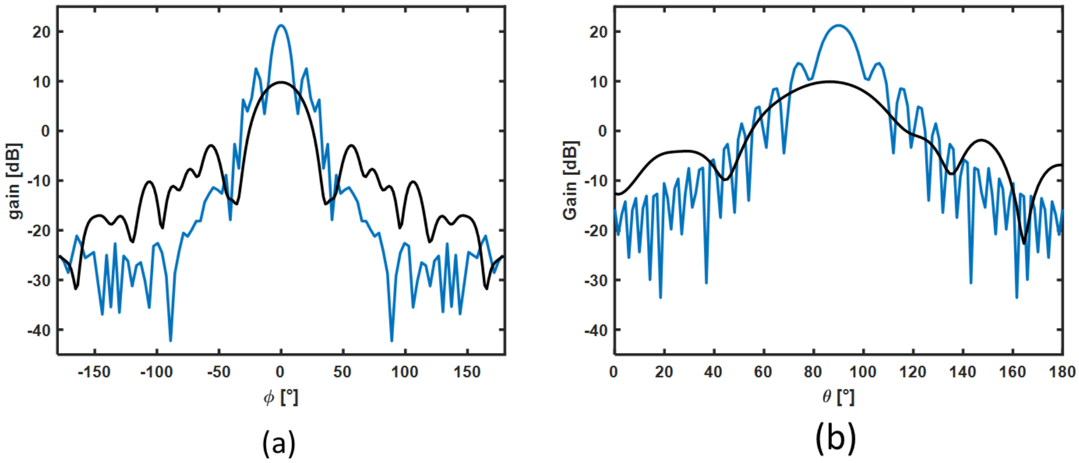

Figure 4. Gain as a function of the angles (a) φ with θ=90° and (b) θ with φ=0° for the plasmonic Vivaldi antenna (black curves) and the all-dielectric Vivaldi antenna (blue curves).

3. CONCLUSIONS

Two different antenna configurations, based on plasmonic and all-dielectric Vivaldi radiators, were investigated by the FDTD simulations. The maximum gain is G=9.9 dB for the plasmonic Vivaldi antenna and G=21.2 dB for the all-dielectric one. The all-dielectric antenna is much more directive than the plasmonic one. However, as a counterpart, its length (L_{aD}=15 µm) is much greater than the one of the plasmonic antenna (L_{aP}=2 µm).
Given the full compatibility of both the antenna configurations with standard SOI waveguides, we can say that they represent two alternative building blocks for OWiNoCs. In particular, the all-dielectric antenna can be preferred for longer range communication (thanks to its higher gain) and when the miniaturization is not a relevant issue in the design of the network topology. Conversely, the plasmonic antenna can be the best choice for improving miniaturization in shorter range communication.

ACKNOWLEDGEMENTS

Research activity supported by MIUR through the PRIN 2015 "Wireless Networks through on-chip Optical Technology - WiNOT" Project. The research is also conducted within the framework of Galileo 2018 G18-625/ PHC Galilée 2018 39622NL.

REFERENCES

[1] A.H. Atabaki, et al.: Integrating photonics with silicon nanoelectronics for the next generation of systems on a chip, *Nature* Vol. 556, pp. 349–353, 2018.
[2] G. Calò, et al, Active InGaAsP/InP photonic bandgap waveguides for wavelength-selective switching, *IEEE Journal of Quantum Electronics*, Vol. 47 (2), pp. 172-181, 2011.
[3] G. Calò, et al, Broadband Mach-Zehnder Switch for Photonic Networks on Chip, J. Lightw. Technol. 30, 944-952 (2012).
[4] B. Alam, et al: Analysis on vertical directional couplers with long range surface plasmons for multilayer optical routing, *Journal of Applied Physics*, Vol. 120 (8), art. no. 083106, 2016.
[5] S. Deb, et al. Wireless NoC as interconnection backbone for multicore chips: Promises and challenges, *IEEE Journal on Emerging and Selected Topics in Circuits and Systems*, Vol. 2, pp. 228–239, 2012.
[6] A. Mineo, et al, Runtime Tunable Transmitting Power Technique in mm-Wave WiNoC Architectures, *IEEE Transactions on Very Large Scale Integration (VLSI) Systems*, vol. 24, no. 4, pp. 1535-1545, 2016.
[7] C. García-Meca, et al: On-chip wireless silicon photonics: From reconfigurable interconnects to lab-on-chip devices, *Light Sci. Appl*., Vol. 6, p. e17053, 2017
[8] G. Bellanca, et al, "Integrated Vivaldi plasmonic antenna for wireless on-chip optical communications," Opt. Express 25, 16214-16227 (2017).
[9] G. Calò, et al: Array of plasmonic Vivaldi antennas coupled to silicon waveguides for wireless networks through on-chip optical technology – WiNOT, *Optics Express*, vol. 26 (23), pp. 30267-30277, 2018.
[10] Lumerical Solutions, Inc. http://www.lumerical.com/tcad-products/fdtd/